

DMD #074740

Title:

**Coproporphyrin-I: A fluorescent, endogenous optimal probe substrate for
ABCC2 (MRP2) that is suitable for vesicle based MRP2 inhibition assay**

Ravindranath Reddy Gilibili, Sagnik Chatterjee, Pravin Bagul, Kathleen W. Mosure, Bokka
Venkata Murali, T. Thanga Mariappan, Sandhya Mandlekar, and Yurong Lai

Pharmaceutical Candidate Optimization, Biocon BMS R&D Center, Syngene International Ltd.,
Bangalore, India (RR, SC, PB, BVM, SM, TM). Pharmaceutical Candidate Optimization, Bristol-Myers
Squibb Company, 3551 Lawrenceville Road, Princeton, NJ 08540 (KM, YL)

DMD #074740

Running title: Coproporphyrin-I as an optimal probe substrate for MRP2 vesicle assay

Corresponding to Sagnik Chatterjee, PhD

Biocon BMS R&D Center, Syngene International Ltd., Bangalore, India

Email: sagnik.chatterjee@syngeneintl.com

Tel. 08066334084

Number of words:

Abstract:	249
Introduction:	747
Discussion:	1460
Number of tables:	1
Number of figures:	4
Number of references:	29

Abbreviations: E17 β G, estradiol-17 β -glucuronide; MRP2, multidrug-resistance associated protein 2; OATP/Oatp, organic anion transporting polypeptide; CP-I, coproporphyrin I; LC-MS/MS, liquid chromatography–tandem mass spectrometry; DJS, Dubin-Johnson syndrome; LTC4, leukotriene C4; ATP, adenosine tri-phosphate; AMP, adenosine mono-phosphate; ABC, ATP binding cassette; BSEP, bile salt export pump; E3S, estrone 3-sulfate; DHEAS, dehydroepiandrosterone sulfate; CDCE, carboxydichlorofluorescein; CDCA, chenodeoxycholic acid; CA, Cholic acid; GCA, Glycocholic acid; TCA, taurocholic acid; TDCA, Taurodeoxycholic acid; DCA, deoxycholic acid; GDCA, glycodeoxycholic acid; GCDCA, glycochenodeoxycholic acid.

DMD #074740

Abstract

Inside-out-oriented membrane vesicles are useful tools to investigate whether a compound can be an inhibitor of efflux transporters such as multidrug-resistance associated protein 2 (MRP2). However, because of technical limitations of substrate diffusion and low dynamic uptake windows for interacting drugs used in clinic, estradiol-17 β -glucuronide (E17 β G) remains the probe substrate frequently used in MRP2 inhibition assays. Here we re-capitulated the sigmoidal kinetics of MRP2 mediated uptake of E17 β G, with apparent K_m and V_{max} values $170 \pm 17 \mu\text{M}$ and $1447 \pm 137 \text{ pmol/mg protein/min}$, respectively. Hill coefficient (2.05 ± 0.1), suggests multiple substrate binding sites for E17 β G transport with cooperative interactions. Using E17 β G as a probe substrate, 51 of 97 compounds tested (53%) showed up to 6-fold stimulatory effects. Alternatively, we demonstrated that coproporphyrin-I (CP-I) is a MRP2 substrate in membrane vesicles, for the first time. The uptake of CP-I followed a hyperbolic relationship, adequately described by the standard Michaelis-Menten equation (apparent K_m and V_{max} values were $7.7 \pm 0.7 \mu\text{M}$ and $48 \pm 11 \text{ pmol/mg protein/min}$, respectively), suggesting the involvement of single binding site. Of 47 compounds tested, thirty compounds were inhibitors of human MRP2 and eight compounds (17%) stimulated MRP2-mediated CP-I transport. The stimulators were found to share basic backbone structure of the physiological steroids, which suggests a potential *in vivo* relevance of *in vitro* stimulation of MRP2 transport. We concluded that CP-I could be an alternative *in vitro* probe substrate replacing E17 β G for appreciating MRP2 interactions while minimizing potential false-negatives for MRP2 inhibition due to stimulatory effects.

DMD #074740

Introduction

Multidrug-resistance associated protein2 (MRP2/*ABCC2*), a member of the ATP-binding cassette (ABC) transporters, is expressed exclusively on the apical membrane of hepatocytes, enterocytes and kidney proximal tubule cells. MRP2 functional deficiency caused by the *ABCC2* gene mutation in human is the molecular basis of conjugated hyperbilirubinemia, known as Dubin-Johnson Syndrome (DJS). MRP2 also transports many structurally diverse drugs and their metabolites and plays a key role in drug disposition and detoxification processes (Nies and Keppler 2007). For example, impaired function of MRP2 could increase the systemic exposure of pravastatin due to the increased absorption and the reduced biliary and/or urinary excretion (Niemi, Arnold et al. 2006). As a result, inhibition of MRP2 can cause accumulation of compounds and/or their metabolites in the liver to reach a toxic level (Isley 2003; Tang 2007). Although drug-drug interactions (DDIs) caused by MRP2 inhibition are still not well-defined in the clinic, given the importance of MRP2 in drug disposition and elimination, it has become one of the emerging transporters of clinical importance as recognized by International Transporter Consortium, ITC (Zamek-Gliszczynski, Hoffmaster et al. 2012; Hillgren, Keppler et al. 2013). ITC has also rationalized the importance of MRP2 in hepatotoxicity due to its role in regulating drug concentration in the liver (Yoshida, Maeda et al. 2013).

As aforementioned, understanding the interaction of a new chemical entity with MRP2 becomes important from DDI and toxicity perspective. Currently two endogenous compounds namely estradiol-17 β -glucuronide (E17 β G) and leukotriene C4 (LTC4) are commonly used in membrane vesicle uptake assays to understand whether a compound is an inhibitor of MRP2 (Brouwer, Keppler et al. 2013). It displays very short duration of uptake linearity (only up to 2 min) in membrane vesicles (Heredi-Szabo, Kis et al. 2008), leading to chances of variability during

DMD #074740

experiments. These limitations hinder the use of LTC₄ in characterizing MRP2 inhibition. As a result, E17βG is the endogenous *in vitro* probe substrate of choice for MRP2 interaction. However, E17βG uptake in membrane vesicles suffers from large inter-laboratory variability in reported *K_m* and *V_{max}* values (Supplemental Table 1) (Borst, Zelcer et al. 2006). E17βG has displayed homotropic cooperativity with MRP2-mediated uptake, yielding sigmoidal kinetics in membrane vesicles (Supplemental Table 1). To explain cooperative interactions, a two-binding-site theory has been proposed for MRP2: E17βG binds to the substrate binding site S that mediates the transport of it, and as E17βG concentration increases it binds to the modulator site M modulating the affinity of the transport site (Figure 1). In addition, complex modulations (stimulation and/or inhibition) of MRP2-mediated E17βG transport have been well-described in the literatures (Bakos, Evers et al. 2000; Evers, Kool et al. 2000; Zelcer, Huisman et al. 2003). The complex modulation suggests that MRP2 interacting compounds could bind to S site to inhibit, or to M sites to stimulate, or both sites to stimulate-and-inhibit MRP2-mediated transport (also known as “bell-shape” kinetics) (Zelcer, Huisman et al. 2003). This stimulatory effect is considered substrate-dependent. For example, probenecid is reported to stimulate E17βG uptake, but inhibits methotrexate uptake in MRP2 membrane vesicles (Zelcer, Saeki et al. 2003). In another study, benzbromarone, sulfasalazine, probenecid and indomethacin are reported to stimulate both human and rat MRP2-mediated E17βG transport, albeit to different extent (Heredi-Szabo, Glavinas et al. 2009). As MRP2-mediated E17βG transport displays sigmoidal kinetics, the self-cooperative effects form a unique interaction for each E17βG-modulator pair within the complex binding sites of MRP2 protein. Therefore, the stimulatory effects could potentially mask the MRP2 inhibition of many modulating compounds and yield false-negative MRP2 inhibition. Collectively, an alternative *in*

DMD #074740

vitro probe substrate that displays classic Michaelis-Menten kinetics is needed for better understanding of MRP2 interactions with new chemical entities.

Coproporphyrin I (CP-I) is one of coproporphyrin byproducts of heme biosynthesis. In the liver, CP-I is taken up into hepatocytes by OATP transporters and effluxed into bile likely by MRP2 (Benz-de Bretagne, Respaud et al. 2011; Benz-de Bretagne, Zahr et al. 2014; Lai, Mandlekar et al. 2016; Shen, Dai et al. 2016). As such, higher proportion of CP-I is secreted in the urine of DJS subjects compared to normal ones. This information indicates a central role of MRP2 in CP-I disposition. However, no *in vitro* corroboration is provided to substantiate these findings to date. In the present study, we aim: (i) to provide a definitive *in vitro* proof of involvement of human MRP2 in transport of CP-I (ii) to characterize in depth the kinetics of CP-I transport in human MRP2 vesicles, and iii) to compare known modulators of hMRP2 in the E17 β G assay, with a special emphasis on reported stimulators.

Materials and Methods

Chemicals and Reagents

Metformin HCl was purchased from RT Corp (WA, USA), Rosuvastatin Calcium was purchased from Angene International Ltd (England, UK). Human MRP2-expressing inside-out membrane vesicles (protein concentration 5 mg/ml) derived from Sf9 insect cells were purchased from GenoMembrane, Co., Ltd (Yokohama, Japan). Reaction incubation plates (96 well, ultra-low attachment, polystyrene, flat bottom, clear) purchased from Corning® Costar® (NY, USA). Assay plates (96 well, black polystyrene) for fluorescence measurement. All other chemicals were purchased from Sigma-Aldrich.

Vesicular Transport Assay

DMD #074740

MRP2-mediate transport assay was performed using inside-out membrane vesicles, according to manufacturer's protocol. Briefly, membrane vesicles were diluted to appropriate concentration with incubation buffer containing 50 mM MOPS-Tris (pH 7.0), 70 mM KCl, 7.5 mM MgCl₂. Diluted membrane vesicles (20µl) were transferred into individual wells of 96-well plate and co-incubated with 0.5 µl of test substrates (CP-I or E17βG) at 37°C for 3 min. Then, the reaction was initiated by adding pre-warmed incubation buffer (29.5 µl) containing with 4 mM ATP or 4 mM AMP and 2mM glutathione. Following incubation for a designated time at 37°C on rotary shaker (Innova 40, New Brunswick Scientific Co., Inc, CT, USA) at 100 rpm, the reaction was stopped by addition of 150 µl cold wash buffer containing 40 mM MOPS-Tris (pH 7.0), 70 mM KCl. The reaction mixture was then transferred into a pre-wet, 96 well filter plate which was placed onto a filtration device (FiltrEX™ 96 Well Filter Plates, Corning Technologies India Pvt Ltd, India), and filtered by a rapid filtration technique (MultiScreen®HTS Vacuum, Manifold, MA, USA). To remove excess reaction mixture, wells were washed for 5 times, each time with 200 µL of ice-cold wash buffer. After the final washing step, the filter plate was dried at room temperature for 1 h. Next, as an extraction solvent, 100 µl of 0.5% SDS dissolved in milliQ water, was added to the filter plate wells and the plate was kept on microplate shaker (VWR, PA, USA) for 15 min at 230 rpm. Then the filter plate was centrifuged (Eppendorf, NY, USA) for 2 min at 778xg along with a receiver plate attached to its bottom to receive the filtrate. In case of E17βG, 100 µl of acetonitrile was used as an extraction solvent. The filtrate was then used to quantify the CP-I or E17βG levels either using a fluorimeter or LC-MS/MS, respectively.

Inhibition of MRP2-Mediated CP-I or E17βG Uptake in Membrane Vesicles

DMD #074740

Various compounds were selected from literature as modulators to evaluate their inhibitory and/or stimulatory effects on MRP2-mediated E17 β G or CP-I transport in membrane vesicles. All modulators were tested at different concentrations. The final assay concentrations of CP-I and E17 β G were 5 and 50 μ M, respectively. For E17 β G as substrate, modulators were tested at 20 and 200 μ M to determine their inhibitory or stimulatory effects on MRP2-mediated transport. With CP-I as substrate, modulators were typically tested at 0.1, 1, 10, 50, 100, 250, 500 and 1000 μ M to determine IC₅₀ values. All compound stock solutions were prepared in DMSO and were spiked directly into assay mixture containing MRP2 vesicle protein (for CP-I and E17 β G are 50 and 25 μ g, respectively), and pre-incubated for 3 min at 37°C. The solubility of inhibitors and stability of the incubation at high concentrations were monitored during the experiments. Then the reaction was initiated with the addition of substrate containing ATP or AMP. The rest of the assay was conducted as described in the above section labelled *vesicular transport assay*. Controls included within each experiment were, with substrate alone (either CP-I or E17 β G) in presence of ATP or AMP. ATP-dependent transport of CP-I or E17 β G was measured in the presence of modulators and compared with control data. The effect of DMSO on the CP-I transport was also evaluated. It was observed that the final DMSO concentrations up to 2% has negligible effect on CP-I transport (data not shown). In this study, DMSO content used was not more than 1.15%.

Fluorimetry Analysis of CP-I

Fluorescence measurements were conducted with microplate reader (SpectraMax® M2e, molecular device), using 401 and 595 nm as excitation and emission wavelengths, respectively for CP-1 ATP-dependent net transport was calculated by subtracting the values obtained in the

DMD #074740

presence of AMP from those in the presence of ATP. All the experiments related to CP-I were conducted in dim light to minimize fluorescent bleaching.

LC-MS/MS Analysis of E17 β G

LC-MS/MS analysis of E17 β G was performed using a Waters UPLC system coupled with Triple Quad 5500 (AB Sciex), fitted with Electro-spray-ionization (ESI) source. Naphthyl glucuronide was used as internal standard (IS). The analyte and IS were separated on a BEH C18-A, 50mm \times 2.1mm column (Waters, USA). An elution gradient with two solvents was used: (A) water with 0.1% formic acid and (B) acetonitrile with 0.1% formic acid. A linear gradient was performed as follows: 0.2 min at 5% solvent B; in 0.5 min solvent B was increased from 5 to 95%, and remained constant at 95% B for 1.20 min. Then in 1.5 min solvent B was decreased from 95 to 5% and it remained constant for 0.5 min. The flow-rate was set at 0.6 mL/min. The ESI source conditions were: capillary voltage, -4500V; drying gas temperature, 450°C; nebulizer gas pressure, 50psi (both nebulizer and drying gas were high-purity nitrogen). E17 β G and IS were monitored in negative ion mode with the transition of m/z 447 \rightarrow 112.7, 547 \rightarrow 112.7, respectively. Analyst v1.6.2 was used for system control and data processing.

Data Analysis

All data were presented as mean \pm SD. Fluorescence intensity from three wells were used to generate mean and SD. To determine the kinetic parameters (K_m and V_{max}) and IC_{50} values, data was analyzed by nonlinear regression using the GraphPad PRISM software version 5.02 (GraphPad Software Inc., San Diego, CA) with following appropriate equations:

DMD #074740

For CP-I, K_m and V_{max} were generated from the direct uptake transport measurements using the Michaelis-Menten equation

$$V = \frac{V_{max} [s]}{K_m + [s]}$$

For E17 β G, the active transport was following sigmoidal fit. Therefore, to obtain best fit Michaelis-Menten equation was modified as given below:

$$V = \frac{V_{max} [s]^h}{K_m^h + [s]^h}$$

Where, V is the velocity (pmol of substrate per milligram of protein per minute), V_{max} is the maximal velocity, $[S]$ is the substrate concentration in μ M, h is Hill coefficient, characterizing the degree of cooperativity and K_m is the Michaelis-Menten constant.

Results

MRP2 Mediated CP-I and E17 β G Transport in Membrane Vesicles

Transport kinetics of E17 β G or CP-I, was first characterized through concentration-dependent transport of E17 β G or CP-I in membrane vesicles overexpressing human MRP2 protein. Prior to the kinetics characterization, ATP-dependent activities and time linearity of MRP2-mediated CP-I uptake were determined at the concentration of 5 μ M for different time-points including 5, 10, 15, 30, 45 and 60 min, at 37°C, in the presence of ATP or AMP. MRP2 mediated CP-I transport in membrane vesicles was linear with time up to 45 min (Supplemental Figure 1). CP-I transport was negligible in the presence of AMP (control) and 35-fold more in the presence of ATP than control. As such, all inhibition studies were optimized to 30 min time-point of

DMD #074740

incubation. For E17 β G, as described previously (Zhang, Han et al. 2016), a 15 min-incubation was chosen as optimal time-point of incubations.

As depicted in Figure 2A, the concentration-dependent MRP2-mediated E17 β G uptake in membrane vesicles appears to follow sigmoidal kinetics with cooperative interaction, which suggests the existence of multiple binding sites. The apparent K_m and V_{max} values (mean \pm S.D) for E17 β G was $170 \pm 17 \mu\text{M}$ and $1447 \pm 137 \text{ pmol/mg protein/min}$, respectively. The Hill coefficient for E17 β G was 2.05 ± 0.1 . In contrast, MRP2 mediated CP-I uptake in membrane vesicles followed a hyperbolic relationship, as the rate of uptake increased in a linear fashion at low concentrations and saturated at high concentrations. The kinetics curve could be adequately modeled by the standard Michaelis-Mention equation (Fig 2B), which suggests the involvement of single binding site in transport of CP-I. The apparent K_m and V_{max} values (mean \pm S.D) for CP-I was $7.7 \pm 0.7 \mu\text{M}$ and $48 \pm 11 \text{ pmol/mg protein/min}$, respectively.

Effects of Modulators on MRP2-Mediated E17 β G Transport in Membrane Vesicles.

In order to investigate the compound dependent stimulation, we tested total of 97 compounds selected from literature to evaluate their effect on E17 β G transport by MRP2 in membrane vesicles. All compounds for E17 β G transport were tested at 20 and 200 μM . Of those compounds tested, 51 compounds displayed stimulatory effects (>10% of control) with at least one concentration (Figure 3 and Supplemental Table 2). Stimulatory effects appeared to be related with concentration of modulators. Mixed effects were also observed, as a subset of compounds showed stimulatory effects at lower concentrations and inhibitory effects at higher concentration, or *vice versa* for other subset molecules (Figure 3).

DMD #074740

Effects of Modulators on MRP2 Mediated CP-I Uptake in Membrane Vesicles

We further tested 47 compounds that either show stimulatory effects in the inhibition of MRP2-mediated E17 β G uptake, or bile acids and statins that share the cholestan structure and are potential stimulators to assess their effects on ATP-dependent CP-I transport by MRP2. The compounds selected were reported in the literature for their inhibitory and/or stimulatory effects on E17 β G transport by MRP2. For example, stimulatory effects of 32 out of 47 compounds selected on MRP2-mediated E17 β G transport were reported in literature (Pedersen, Matsson et al. 2008; Morgan, van Staden et al. 2013). In addition, a few representative statins, bile acids and steroidal compounds were also included to test their effects on CP-I uptake transport by MRP2.

Of the compounds assessed, 30 compounds were determined as inhibitors for MRP2-mediated CP-I transport (Table 1). Of 30 inhibitors, 7 compounds were obtained with IC_{50} <100 μ M, ranging from 11 to 84 μ M as benzbromarone > bromosulphothalein > MK-571 > troglitazone > rifampicin > atorvastatin > losartan potassium. Ten compounds, including nodolol, alpha-bilirubin, metformin, acetaminophen, TCA and CA displayed no effect on ATP-dependent CP-I uptake transport by MRP2. Eight compounds (17%) were identified as stimulators, as compared to 32 compounds out of 47 when E17 β G was used as the probe substrate. The net changes in stimulation with these compounds varied from 34% to 181% (Table 1). “Bell-shaped” inhibition curve of MRP2-mediated CP-I transport was observed with E17 β G, appearing stimulatory effects at low concentrations (0.1 to 100 μ M) and inhibitory effects at high concentrations e.g >100 μ M, with IC_{50} value of 187 μ M.

Structure Similarity of Stimulators of MRP2 Mediated CP-I Uptake in Membrane Vesicles

DMD #074740

The chemical structures of the stimulators of MRP2 mediated CP-I uptake in membrane vesicles are depicted in Figure 5. These stimulators, except for mitoxantrone and pyrimethamine, share the general pattern of the 17-carbon ring backbone, which is the same structure used by other biologically important steroid molecules including steroid hormones, bile acids and vitamins (Figure 5). Mitoxantrone has two identical side chains containing both amino and hydroxyl-moieties with rich in oxygen- and nitrogen-containing planar tricyclic anthraquinone rings (pKa 9.08). Pyrimethamine (pKa 7.34) belongs to phenylpyrimidines that contain a benzene ring linked to a pyrimidine ring through a CC or CN bound (Figure 5).

Discussion

ABC transporter MRP2 transports its substrates from the inside to the outside of cells. As a result, identifying a substrate in an intact cell system overexpressing MRP2 protein is difficult through monitoring direct transport of the substrate. Alternatively, substrate transport can be determined using inside-out-oriented membrane vesicles demonstrating ATP-dependent transport of a substrate into the vesicles. For inhibition studies, ideally probe substrates should be potential victim drugs used in clinic. However, due to technical difficulties such as extensive substrate diffusion into membrane vesicles, lack of optimal dynamic window of ATP-dependent uptake, make most xenobiotic substrates unsuitable in the vesicle assay. Currently LTC₄ and E17βG are recommended by ITC as probe substrates for assessing MRP2 inhibition (Brouwer, Keppler et al. 2013).

DMD #074740

In the present study, we first tested 97 compounds in MRP2 mediated E17 β G transport at two concentrations, 20 and 200 μ M (Figure 3 and 4). Of these, 51 compounds (53%) were found to be the stimulators of MRP2-mediated E17 β G transport at least one of the two concentrations tested. Our data are in good agreement with results reported previously, where in most instances, marketed drugs have been shown to stimulate the MRP2-mediated E17 β G transport (Pedersen, Matsson et al. 2008; Morgan, van Staden et al. 2013). For some compounds (dacarbazine and sulfasalazine), a strong stimulation was observed at lower concentration (20 μ M), while E17 β G transport was inhibited at high concentrations (200 μ M), demonstrating “bell-shape” of modulation. The stimulatory effects of compounds on MRP2-mediated E17 β G transport in membrane vesicles limits the use of E17 β G, as concerns of false negative inhibition remain for many modulating compounds. The concern for false negative becomes important in explaining hyperbilirubinemia caused by MRP2 inhibition. A compound can cause hyperbilirubinemia by causing direct hepatotoxicity or by inhibiting MRP2-mediated bilirubin transport. Hyperbilirubinemia mediated by MRP2 inhibition, may not be fatal for the progression of the compound down clinical development, however hepatotoxicity signal can prevent a compound from further progress. Therefore, providing a clinically relevant MRP2 probe, devoid of the risk of identifying a compound as false negative becomes very important for progressing a compound further. In this relation, CP-I as probe substrate identified 64% of the 47 compounds, as inhibitors (Figure 4). This will help to differentiate hyperbilirubinemia as a consequence of MRP2 inhibition from hyperbilirubinemia via hepatotoxicity. In contrast, using E17 β G as probe substrate, it is difficult to classify compounds as inhibitors, as compounds vary significantly in their behavior depending on concentration (bell shaped curves). Therefore, in our study, we separated the

DMD #074740

compounds as stimulators and ‘inhibitors and/no effects’ based on their behavior using E17 β G as probe substrate (Figure 4).

Although the urinary concentration ratio of CP-I to that of sum of CP-I and CP-III has been used as a surrogate marker to assess MRP2 activity clinically (Benz-de Bretagne, Respaud et al. 2011), *in vitro* evidence of transport of CP-I by MRP2 was lacking. Herein, we have shown for the first time that CP-I is taken up into membrane vesicles overexpressing MRP2, and the ATP dependent uptake was about 30-fold higher than control, which provided an excellent dynamic window to assess MRP2 inhibitory effects. In addition, the transport of CP-I by MRP2 was linear up to 45 min (Supplemental Figure 1), which provides a time range enough to decrease variations, as compared to LTC₄ (Heredi-Szabo, Kis et al. 2008). Low K_m of LTC₄ (695 μ M) deviates its uptake from linearity very quickly, making results with it prone to variations. In addition, CP-I being fluorescent, is easily measurable, compared to LTC₄ which requires radioactivity analysis. In addition to LTC₄, carboxy-dichlorofluorescein (CDF) is also recommended as a probe substrate for MRP2 by ITC (Brouwer, Keppler et al. 2013). CDF follows a Michaelis-Menten kinetics and is a fluorescent substrate, however it is not endogenous. CDF is administered in cell system as diacetate prodrug (CDFDA), as CDF is a poor permeable molecule. CDF transport is also reported to be stimulated by different compounds such as verapamil, budesonide and thioridazine (Munic, Hlevnjak et al. 2011; Kidron, Wissel et al. 2012). However, it is challenging to further understand the significance of stimulation of MRP2-mediated CDF transport *in vivo*, because of the permeability and prodrug factor.

Unlike E17 β G, CP-I uptake in MRP2 expressed membrane vesicles followed a Michaelis-Menten kinetics (Figure 2B), which indicates that CP-I does not have affinity for the modulator site, for its own transport. Most importantly, although 32 out of the 47 compounds, chosen to

DMD #074740

assess CP-I transport, are identified as stimulators in E17 β G transport (Figure 3), either in literature (Pedersen, Matsson et al. 2008; Morgan, van Staden et al. 2013), or in our data; only 8 compounds were found to stimulate CP-I transport. Therefore, with CP-I as probe substrate, the percentage of compound showing *in vitro* stimulation, was largely reduced. While stimulators of E17 β G transport varied widely in their structural features, stimulators of CP-I transport displayed common structural feature of 17 carbon ring steroid moiety (Figure 5). The two other compounds, mitoxantrone and pyrimethamine are strongly basic. Mitoxantrone forms a head-to-tail dimer and binds at two opposite grooves of the G-quadruplex. These structural features are being investigated with *in vivo* studies to understand the physiological relevance of the stimulators with structure similarities.

E17 β G kinetics is usually explained by distinct modulator and transport sites (Zelcer, Huisman et al. 2003; Borst, Zelcer et al. 2006). The substantial stimulatory effect of binding of E17 β G to the modulator site, changes the transport kinetics to sigmoidal nature. However, E17 β G stimulated the transport of CP-I only to a low extent (< 40% till 10 μ M, while E17 β G was an inhibitor of CP-I transport at higher concentrations). Therefore, an assumption can be made that the binding of E17 β G to the modulator site has a minimum effect on transport of CP-I. This proves that the stimulation is a probe substrate dependent phenomena, further proving the importance for a clinically relevant probe substrate.

Among the compounds assessed, bile acids inhibited MRP2-mediated CP-I transport. Previous studies indicated GCDCA, TCDCA, TDCA and GCA as stimulators of MRP-2 mediated E17 β G transport (Bodo, Bakos et al. 2003). With CP-I as substrate, CDCA, DCA, GCDCA, GDCA, and TDCA were found to be inhibitors of MRP2. MRP2 is responsible for bile acid-independent bile flow in case of cholestasis. As a result, accumulated intra-hepatic bile acids due

DMD #074740

to cholestasis might inhibit MRP2 function, and result in hyperbilirubinemia, providing another mechanism of bilirubin increase, apart from direct hepatotoxicity.

Although diclofenac, indomethacin, glyburide, losartan and troglitazone are stimulators of E17 β G transport (Figure 3) (Morgan, van Staden et al. 2013), these compounds appeared to be inhibitors in MRP2 mediated CP-I transport (Table 1). Troglitazone was withdrawn from the market for cases of liver failure. Cholestasis mediated by bile salt export pump (BSEP/*ABCB11*) inhibition and reactive metabolite formation from troglitazone sulfate has been shown to be two major mechanism of toxicity. Although it has been reported to downregulate MRP2 expression (Foster, Jacobsen et al. 2012), MRP2 functional inhibition by troglitazone can potentially contribute to the observed cholestatic injury with troglitazone. In addition, troglitazone sulfate is reported to be more potent inhibitor of canalicular transporter BSEP and hence its hepatic accumulation increases the toxicity (Funk, Pantze et al. 2001). Troglitazone sulfate is also reported to be a substrate of MRP2 (Kostrubsky, Vore et al. 2001). Troglitazone, by inhibiting MRP2 can contribute to higher accumulation of troglitazone sulfate and hence toxicity. Higher intrahepatic levels of troglitazone sulfate corroborates our findings (Chojkier 2005). Therefore, interaction of troglitazone sulfate with MRP2 and its contribution to the accumulation of troglitazone and its sulfate conjugates remains to be further determined. Similarly, losartan and glyburide are drugs associated with clinical liability of liver toxicity. They are reported to be MRP2 inhibitors in our study for the first time. Although the relationship of MRP2 inhibition and liver toxicity remains to be further explored, our data could shed a new light into the mechanism of hepatotoxicity caused by troglitazone, losartan and glyburide.

To summarize, in order to better understand MRP2 inhibition and the *in vivo* consequence, an alternative *in vitro* probe substrate is needed to minimize the stimulatory effects and consequent

DMD #074740

false negative occurrences in membrane vesicle assays using E17 β G as a substrate. Herein, we have for the first time shown CP-I to be a MRP2 *in vitro* substrate for appreciating MRP2 inhibition. The transport kinetics were obtained in membrane vesicles transfected with MRP2. Only eight compounds with structural similarity stimulated CP-I transport among 47 compounds evaluated. With CP-1, previously classified stimulators including diclofenac, indomethacin, glyburide, losartan and troglitazone in MRP2-mediated E17 β G vesicle uptake, were now re-determined to be potent MRP2 inhibitors. In addition, bile acids and atorvastatin, simvastatin, lovastatin and rosuvastatin were also found to be inhibitors of MRP2 mediated CP-I transport. We conclude that CP-I is a better probe substrate in membrane vesicle uptake assays for characterizing MRP2-inhibition effects.

DMD #074740

Acknowledgments

We would like to thank Punit Marathe, William Humphreys, Devang Shah, Murali Subramanian, and Mike Sinz during various aspects of this work, e.g. data analysis, experimental set up, reviewing manuscript.

Authorship Contributions

Participated in research design: YL, SC, RR.

Conducted experiments: RR, SC, KM, PB, BVM

Contributed new reagents or analytic tools: RR, SC, PB, KM

Performed data analysis: YL, RR, SC, PB, KM, TM

Wrote or contributed to the writing of the manuscript: YL, SC, RR, KM, PB, TM, SM.

DMD #074740

References

- Bakos, E., R. Evers, et al. (2000). "Interactions of the human multidrug resistance proteins MRP1 and MRP2 with organic anions." Mol Pharmacol **57**(4): 760-768.
- Benz-de Bretagne, I., R. Respaud, et al. (2011). "Urinary elimination of coproporphyrins is dependent on ABCB2 polymorphisms and represents a potential biomarker of MRP2 activity in humans." J Biomed Biotechnol **2011**: 498757.
- Benz-de Bretagne, I., N. Zahr, et al. (2014). "Urinary coproporphyrin I/(I + III) ratio as a surrogate for MRP2 or other transporter activities involved in methotrexate clearance." Br J Clin Pharmacol **78**(2): 329-342.
- Bodo, A., E. Bakos, et al. (2003). "Differential modulation of the human liver conjugate transporters MRP2 and MRP3 by bile acids and organic anions." J Biol Chem **278**(26): 23529-23537.
- Borst, P., N. Zelcer, et al. (2006). "MRP2 and 3 in health and disease." Cancer Lett **234**(1): 51-61.
- Brouwer, K. L., D. Keppler, et al. (2013). "In vitro methods to support transporter evaluation in drug discovery and development." Clin Pharmacol Ther **94**(1): 95-112.
- Chojkier, M. (2005). "Troglitazone and liver injury: in search of answers." Hepatology **41**(2): 237-246.
- Evers, R., M. Kool, et al. (2000). "Inhibitory effect of the reversal agents V-104, GF120918 and Pluronic L61 on MDR1 Pgp-, MRP1- and MRP2-mediated transport." Br J Cancer **83**(3): 366-374.
- Foster, J. R., M. Jacobsen, et al. (2012). "Differential effect of troglitazone on the human bile acid transporters, MRP2 and BSEP, in the PXB hepatic chimeric mouse." Toxicol Pathol **40**(8): 1106-1116.
- Funk, C., M. Pantze, et al. (2001). "Troglitazone-induced intrahepatic cholestasis by an interference with the hepatobiliary export of bile acids in male and female rats. Correlation with the gender difference in troglitazone sulfate formation and the inhibition of the canalicular bile salt export pump (Bsep) by troglitazone and troglitazone sulfate." Toxicology **167**(1): 83-98.
- Heredi-Szabo, K., H. Glavinas, et al. (2009). "Multidrug resistance protein 2-mediated estradiol-17beta-D-glucuronide transport potentiation: in vitro-in vivo correlation and species specificity." Drug Metab Dispos **37**(4): 794-801.
- Heredi-Szabo, K., E. Kis, et al. (2008). "Characterization of 5(6)-carboxy-2',7'-dichlorofluorescein transport by MRP2 and utilization of this substrate as a fluorescent surrogate for LTC4." J Biomol Screen **13**(4): 295-301.
- Hillgren, K. M., D. Keppler, et al. (2013). "Emerging transporters of clinical importance: an update from the International Transporter Consortium." Clin Pharmacol Ther **94**(1): 52-63.
- Isley, W. L. (2003). "Hepatotoxicity of thiazolidinediones." Expert Opin Drug Saf **2**(6): 581-586.
- Kidron, H., G. Wissel, et al. (2012). "Impact of probe compound in MRP2 vesicular transport assays." Eur J Pharm Sci **46**(1-2): 100-105.
- Kostrubsky, V. E., M. Vore, et al. (2001). "The effect of troglitazone biliary excretion on metabolite distribution and cholestasis in transporter-deficient rats." Drug Metab Dispos **29**(12): 1561-1566.

DMD #074740

- Lai, Y., S. Mandlekar, et al. (2016). "Coproporphyrins in Plasma and Urine Can Be Appropriate Clinical Biomarkers to Recapitulate Drug-Drug Interactions Mediated by Organic Anion Transporting Polypeptide Inhibition." J Pharmacol Exp Ther **358**(3): 397-404.
- Morgan, R. E., C. J. van Staden, et al. (2013). "A multifactorial approach to hepatobiliary transporter assessment enables improved therapeutic compound development." Toxicol Sci **136**(1): 216-241.
- Munic, V., M. Hlevnjak, et al. (2011). "Characterization of rhodamine-123, calcein and 5(6)-carboxy-2',7'-dichlorofluorescein (CDCF) export via MRP2 (ABCC2) in MES-SA and A549 cells." Eur J Pharm Sci **43**(5): 359-369.
- Niemi, M., K. A. Arnold, et al. (2006). "Association of genetic polymorphism in ABCC2 with hepatic multidrug resistance-associated protein 2 expression and pravastatin pharmacokinetics." Pharmacogenet Genomics **16**(11): 801-808.
- Nies, A. T. and D. Keppler (2007). "The apical conjugate efflux pump ABCC2 (MRP2)." Pflugers Arch **453**(5): 643-659.
- Pedersen, J. M., P. Matsson, et al. (2008). "Prediction and identification of drug interactions with the human ATP-binding cassette transporter multidrug-resistance associated protein 2 (MRP2; ABCC2)." J Med Chem **51**(11): 3275-3287.
- Shen, H., J. Dai, et al. (2016). "Coproporphyrins I and III as Functional Markers of OATP1B Activity: In Vitro and In Vivo Evaluation in Preclinical Species." J Pharmacol Exp Ther **357**(2): 382-393.
- Tang, W. (2007). "Drug metabolite profiling and elucidation of drug-induced hepatotoxicity." Expert Opin Drug Metab Toxicol **3**(3): 407-420.
- Yoshida, K., K. Maeda, et al. (2013). "Hepatic and intestinal drug transporters: prediction of pharmacokinetic effects caused by drug-drug interactions and genetic polymorphisms." Annu Rev Pharmacol Toxicol **53**: 581-612.
- Zamek-Gliszczynski, M. J., K. A. Hoffmaster, et al. (2012). "Highlights from the international transporter consortium second workshop." Clin Pharmacol Ther **92**(5): 553-556.
- Zelcer, N., M. T. Huisman, et al. (2003). "Evidence for two interacting ligand binding sites in human multidrug resistance protein 2 (ATP binding cassette C2)." J Biol Chem **278**(26): 23538-23544.
- Zelcer, N., T. Saeki, et al. (2003). "Transport of bile acids in multidrug-resistance-protein 3-overexpressing cells co-transfected with the ileal Na⁺-dependent bile-acid transporter." Biochem J **369**(Pt 1): 23-30.
- Zhang, Y., Y. H. Han, et al. (2016). "Diclofenac and Its Acyl Glucuronide: Determination of In Vivo Exposure in Human Subjects and Characterization as Human Drug Transporter Substrates In Vitro." Drug Metab Dispos **44**(3): 320-328.

DMD #074740

Footnote:

Yurong Lai: Current address: Drug Metabolism, Gilead Sciences, Inc. 333 Lakeside Drive, Foster City, CA 94404, USA. Email Yurong.lai@gilead.com

Figure legends:

Figure 1. Scheme of two binding-sites model for MRP2.

Substrates or modulating compounds bind to the substrate binding site S that mediates the transport of the substrate, and can also bind to the modulator site M that modulate the affinity of the transport site. The proposed mechanism of E17 β G is that, it first binds to S site, followed by M site at higher concentration, resulting in sigmoidal kinetics.

Figure 2. Concentration-dependent uptake transport of E17 β G (A) and CP-I (B) in MRP2-expressing Sf9 membrane vesicles.

MRP2 membrane vesicles were incubated at 37°C for 15 min (E17 β G) or 30 mins (CP-I). ATP-dependent uptake is measured by subtracting uptake in the presence of AMP from that of ATP. For MRP2-mediated E17 β G uptake, K_m and V_{max} values were $170 \pm 17 \mu\text{M}$ and $1447 \pm 137 \text{ pmol/mg protein/min}$, respectively. Hill plot was shown as insert graph and Hill coefficient is 2.046 ± 0.1 . For MRP2 mediated CP-I uptake, K_m and V_{max} values were $7.7 \pm 0.7 \mu\text{M}$ and $48 \pm 11 \text{ pmol/mg protein/min}$, respectively. Hill coefficient is 1 for the best fit. The data are presented as mean and SD of a single experiment performed in triplicate.

DMD #074740

Figure 3: Graphical representation of effect of various modulators on MRP2-mediated E17 β G transport. MRP2-mediated E17 β G transport was measured in inside-out membrane vesicles, derived from MRP2 expressing Sf9 insect cells, after incubation with E17 β G at 50 μ M with and without modulators at 20 and 200 μ M. A total of 96 modulators were tested, among these 51 modulators (53 %) stimulated MRP2-mediated E17 β G transport by $\geq 10\%$. 16 modulators (16%) significantly inhibited E17 β G transport at least either one or both of the concentrations tested. The data was presented as mean from a single experiment (CV% $<20\%$).

Figure 4: Graphical representation of modulators of E17 β G and CP-I transport

Pie chart of the segregation of compounds based on their transport properties with either 50 μ M E17 β G (A) or 5 μ M CP-I (B), in MRP2 transfected Sf9 membrane vesicles. For E17 β G transport, compounds were classified in two classes: stimulators (showing $> 10\%$ stimulation of E17 β G transport) and no effect/inhibitors; for CP-I transport, compounds were classified in three classes, inhibitors, stimulators and compounds with no effect.

Figure 5: chemical structure of stimulators for MRP2-mediated CP-I transport

DMD #074740

Table 1. List of compounds tested for their modulatory effect against CP-I as substrate, and their classification into type of modulator: compounds with no modulation are listed first, followed by inhibitors in order of increasing IC₅₀, followed by stimulators.

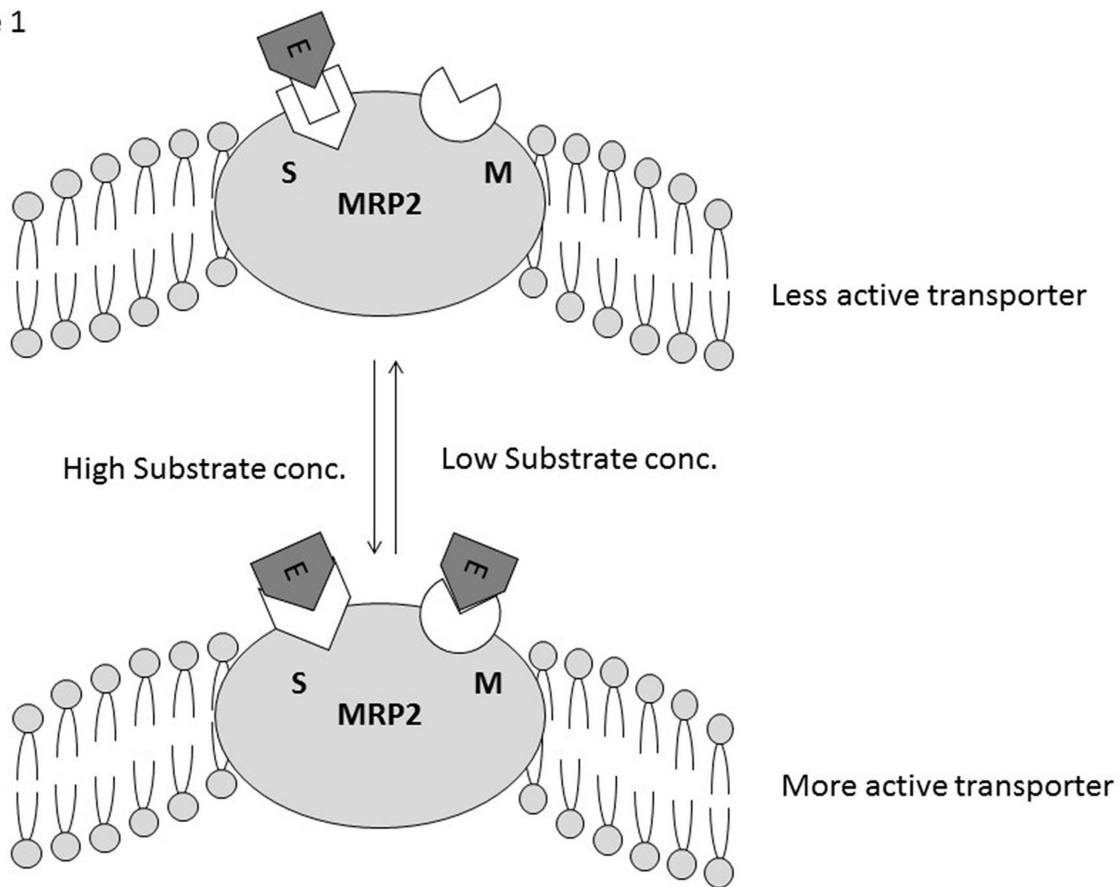
Compound	Type of modulator	IC50 (µM) Mean±SD	Comments	Compound	Type of modulator	IC50 (µM) Mean±SD	Comments
Acetaminophen	None	ND	No effect	E17bG	Inhibitor/stimulator	188 ± 32	Moderate inhibitor; Maximum net stimulation 39% at 1µM
Etoposide	None	ND	No effect	Indomethacin	Inhibitor	214 ± 14	Weak Inhibitor
Nadolol	None	ND	No effect	TDCA	Inhibitor	218 ± 22	Weak Inhibitor
Tolbutamide	None	ND	No effect	Lovastatin	Inhibitor	217 ± 9	Weak Inhibitor
Alpha-Bilirubin	None	ND	No effect	DCA	Inhibitor	212 ± 2	Weak Inhibitor
CA	None	ND	No effect	Glyburide	Inhibitor	210 ± 79	Weak Inhibitor
GCA	None	ND	No effect	Glimpride	Inhibitor	305 ± 43	Weak Inhibitor
TCA	None	ND	No effect	GDC A	Inhibitor	325 ± 20	Weak Inhibitor
Pravastatin	None	ND	No effect	GCDCA	Inhibitor	410 ± 40	Weak Inhibitor
Metformin	None	ND	No effect	Rosuvastatin	Inhibitor	412 ± 183	Weak Inhibitor
Benzbromarone	Inhibitor	11 ± 0.5	Strong inhibitor	Irinotecan	Inhibitor	532 ± 171	Weak Inhibitor
Bromosulphothalein	Inhibitor	26 ± 2	Strong inhibitor	Bumetanide	Inhibitor	541 ± 172	Weak Inhibitor
MK-571	Inhibitor	39 ± 3	Strong inhibitor	Gemfibrozil	Inhibitor	648 ± 71	Weak Inhibitor
Troglitazone	Inhibitor	53 ± 3	Strong inhibitor	Phenylbutazone	Inhibitor	777 ± 47	Weak Inhibitor
Rifamycin SV	Inhibitor	59 ± 1	Strong inhibitor	Nimodipine	Inhibitor	793 ± 35	Weak Inhibitor

DMD #074740

Atorvastatin	Inhibitor	60 ± 3	Strong inhibitor	Probenecid	Inhibitor	110 ± 67	Weak Inhibitor
Losarton Potassium	Inhibitor	74 ± 3	Strong inhibitor	Budesonide	Stimulator	ND	Maximum net stimulation 82% at 250µM
Rifampicin	Inhibitor	83 ± 8	Strong inhibitor	DHA3S	Stimulator	ND	Maximum net stimulation 62% at 100µM
CDCF	Inhibitor	130 ± 20	Moderate inhibitor	Mitoxantrone	Stimulator	ND	Maximum net stimulation 180% at 100µM
Simvastatin	Inhibitor	132 ± 24	Moderate inhibitor	Progesterone	Stimulator	ND	Maximum net stimulation 95% at 50µM
Terfenadine	Inhibitor	150 ± 2	Moderate inhibitor	Testosterone	Stimulator	ND	Maximum net stimulation 79% at 100µM
Sulfasalazine	Inhibitor	161 ± 45	Moderate inhibitor	E3S	Stimulator	ND	Maximum net stimulation 34% at 100µM
Diclofenac	Inhibitor	168 ± 14	Moderate inhibitor				
CDCA	Inhibitor	175 ± 21	Moderate inhibitor	Pyrimethamine	Stimulator	ND	Maximum net stimulation 49% at 1µM

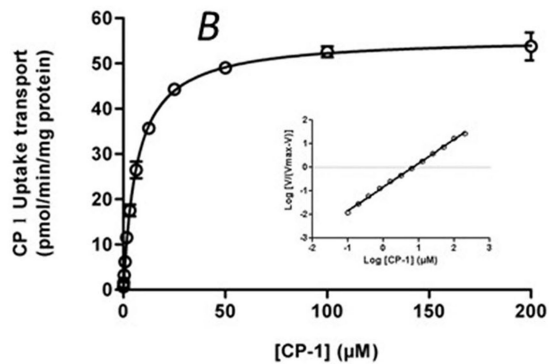
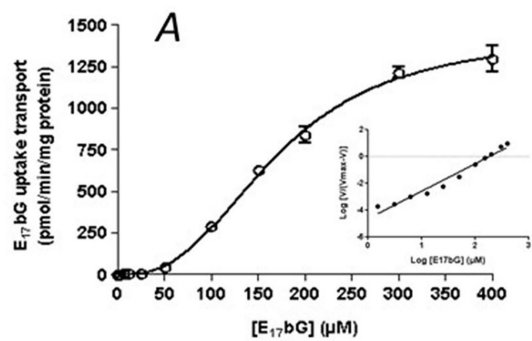
ND: not determined; Strong inhibitors IC₅₀<100µM; Moderate inhibitors IC₅₀=100 to 200µM; Weak inhibitors IC₅₀>200µM.

Figure 1



E: Estradiol-17b-glucuronide, S: substrate binding site, M: Modulator binding site

Figure 2



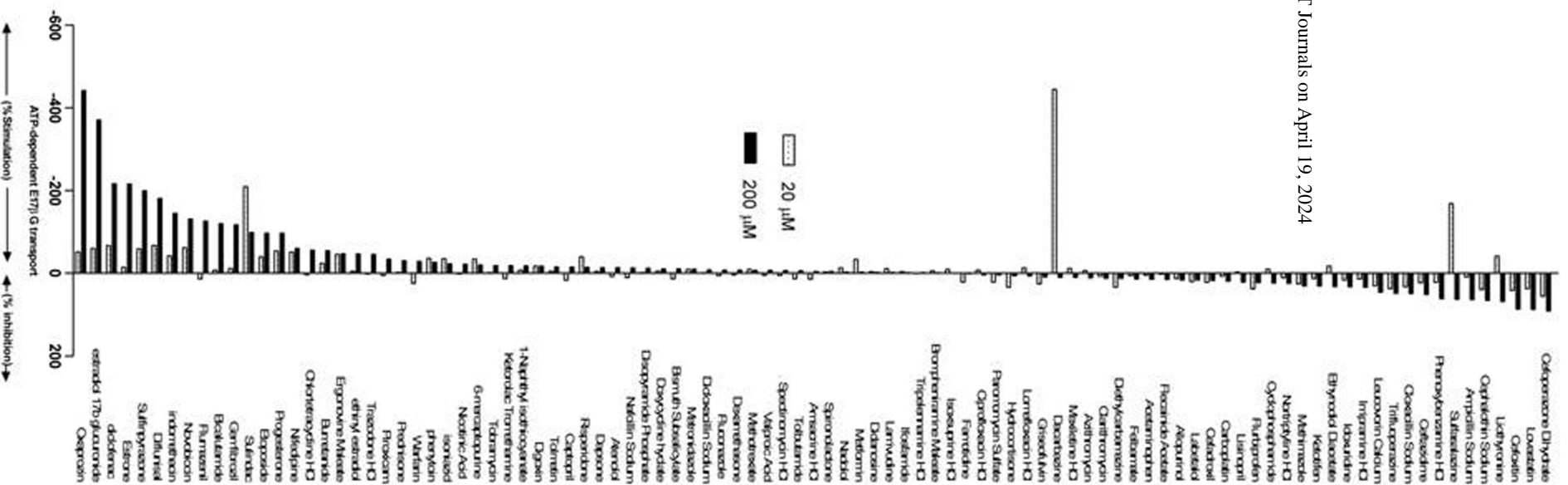
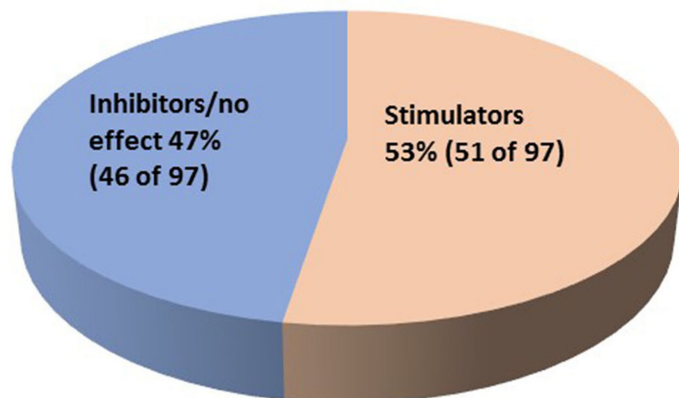


Figure 4

Modulators	Number of compounds	
	E17bG	CP-I
Inhibitors	-	30
Stimulators	51	8 (E17bG included)
No effect/Inhibitors	46	10
Total	97	47

E17bG



CP-I

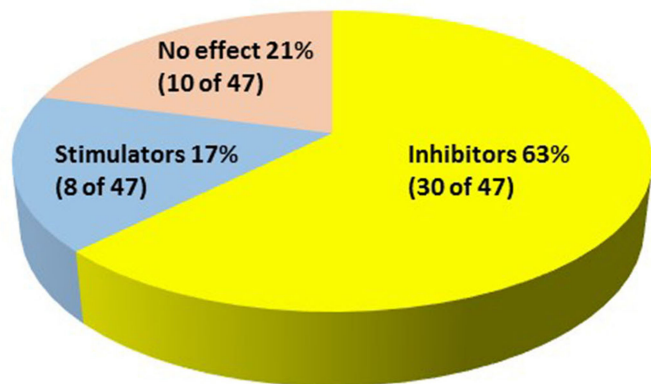
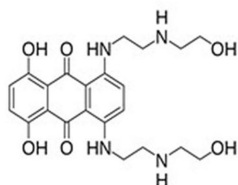
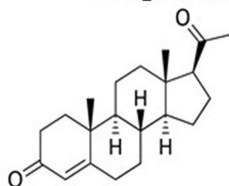


Figure 5

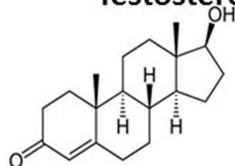
Mitoxantrone



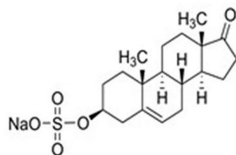
Progesterone



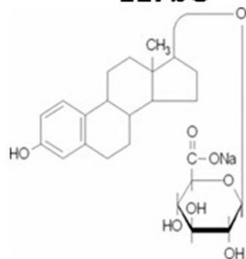
Testosterone



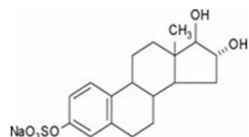
DHA3S



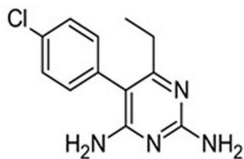
E17bG



E3S



Pyrimethamine



Budesonide

